

The Striking Influence of Intramolecular Lanthanoid– π –Arene Interactions on the Structural Architecture of the Homoleptic Aryloxolanthanoid(II) Complexes $[\text{Eu}_2(\text{Odpp})(\mu\text{-Odpp})_3]$ and $[\text{Yb}_2(\text{Odpp})_2(\mu\text{-Odpp})_2]$ and the Yb^{II}/Yb^{III} Trimetallic $[\text{Yb}_2(\mu\text{-Odpp})_3]^+[\text{Yb}(\text{Odpp})_4]^-$ ($-\text{Odpp} = 2,6\text{-Diphenylphenolate}$)

Glen B. Deacon,^{*,[a]} Craig M. Forsyth,^[a] Peter C. Junk,^[b] Brian W. Skelton,^[c] and Allan H. White^[c]

Abstract: Homoleptic binuclear aryloxolanthanoid(II) complexes, $[\text{Eu}_2(\text{Odpp})(\mu\text{-Odpp})_3]$ (**1**) ($-\text{Odpp} = 2,6\text{-diphenylphenolate}$), $[\text{Yb}_2(\text{Odpp})_2(\mu\text{-Odpp})_2]$ (**2**) and the remarkable mixed-valent complex $[\text{Yb}_3(\text{Odpp})_7]$ (**3**), have been prepared by direct reactions of ytterbium or europium metal with 2,6-diphenylphenol in the presence of mercury at elevated temperatures in sealed tubes. X-ray diffraction studies of **1** and **2** (as toluene solvates from extraction of reaction mixtures) revealed different binuclear structures. In **1** three aryloxide oxygens bridge the two Eu atoms, with a

terminal Odpp and three $\eta^1\text{-}\pi$ -bonded substituent phenyl groups also attached to one Eu, and three $\eta^2\text{-}\pi$ -bonded phenyl groups to the other. By contrast, both Yb atoms of **2** have one terminal and two bridging Odpp ligands in a pyramidal array and the coordination sphere is completed by π interactions of pendant phenyl groups (one η^4 - and one η^3 - to one Yb, and an η^6 - and an $\eta^1\text{-Ph}$

group to the other). The structure of **3** comprises an unprecedented $[\text{Yb}^{\text{II}}(\text{Odpp})_3]^+$ cation and a $[\text{Yb}^{\text{III}}(\text{Odpp})_4]^-$ anion. In the cation, there are solely three bridging aryloxide ligands with additional coordination of one η^6 - and two $\eta^1\text{-}\pi\text{-Ph}$ groups at one Yb and one η^6 -, one η^2 - and one $\eta^1\text{-Ph}$ at the other. The $[\text{Yb}(\text{Odpp})_4]^-$ anion has a near-tetrahedral arrangement of four aryloxide oxygens. In **1**, **2**, and **3**, naked lanthanoid coordination sites and faces are protected by bulky pendant phenyl groups with concomitant $\pi\text{-Ph-Ln}$ interactions.

Keywords: europium • lanthanides • mixed-valent compounds • O ligands • ytterbium

Introduction

Over the past decade, there has been significant interest in low-coordination-number (≤ 6) lanthanoid complexes.^[1] The large and electropositive lanthanoid cations generally achieve stability through high coordination numbers, either by bonding to auxiliary neutral molecules—usually O- or N-donor solvents—or by generating oligomeric arrays. Thus, the imposition of an unfavourable, low-coordinate environment upon the lanthanoid centre can lead to unusual structures and

novel lanthanoid–ligand interactions, for example with hydrocarbon fragments.^[1] The use of aryloxide ligands (OAr , e.g. $\text{Ar} = \text{C}_6\text{H}_2\text{-}2,6\text{-}t\text{Bu}_2\text{-}4\text{-R}$,^[2] $\text{C}_6\text{H}_3\text{-}2,6\text{-}i\text{Pr}_2$ ^[3] or $\text{C}_6\text{H}_3\text{-}2,6\text{-Ph}_2$ ^[4]) has allowed isolation of *solvent-free* lanthanoid(III) aryloxides, $[\text{Ln}(\text{OAr})_3]$. The sterically demanding 2,6-substituents can effectively inhibit oxygen bridging since, in dimeric $[\{\text{Ln}(\text{OC}_6\text{H}_3\text{-}2,6\text{-}i\text{Pr}_2)_3\}_2]$, the two monomeric $\text{Ln}(\text{OAr})_3$ units are linked by $\eta^6\text{-arene-lanthanoid}$ interactions.^[3] The bulkier *tert*-butyl substituents in $[\text{Ln}(\text{OC}_6\text{H}_3\text{-}2,6\text{-}t\text{Bu}_2\text{-}4\text{-R})_3]$ can completely block the coordination sphere of the lanthanoid, giving monomeric, three-coordinate complexes.^[2] In lanthanoid(II) chemistry the only example of a solvent-free aryloxide is $[\text{Yb}(\text{OC}_6\text{H}_2\text{-}2,6\text{-}t\text{Bu}_2\text{-}4\text{-Me})_2]$.^[5] In this case, a dimeric structure results in which the ytterbium centres are three-coordinate with oxygen-bridged aryloxides. Similar structures are also observed in bulky ytterbium aryloxide/amide systems.^[5a] We have shown previously for $[\text{Ln}(\text{Odpp})_3]$ complexes that the primary coordination by the three aryloxide oxygens is supplemented by weaker intramolecular $\pi\text{-phenyl-lanthanoid}$ interactions.^[4] The latter can effectively replace coordination of up to two tetrahydrofuran

[a] Prof. G. B. Deacon, Dr. C. M. Forsyth
Chemistry Department, Monash University
Clayton, Victoria 3168 (Australia)
Fax: (+61) 3-9905-4597
E-mail: glen.deacon@sci.monash.edu.au

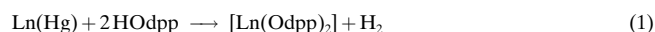
[b] Dr. P. C. Junk
Department of Chemistry, James Cook University
Townsville, Queensland 4811 (Australia)

[c] Dr. B. W. Skelton, Prof. A. H. White
Department of Chemistry, The University of Western Australia
Nedlands, Western Australia 6907 (Australia)

(THF) molecules, as exemplified by the series [Nd(Odpp)₃(thf)₂](thf)₂ (CN = 5, no Ph–Ln interaction), [Nd(Odpp)₃(thf)] (CN = 4, with one η³-Ph–Ln interaction) and [Nd(Odpp)₃] (CN = 3, with one η¹- and one η⁶-Ph–Ln interaction).^[4b] We have now investigated lanthanoid(II) 2,6-diphenylphenolates [Ln(Odpp)₂], where intramolecular π-Ph–Ln interactions may assume even greater significance because of the lower Odpp/Ln ratio and the relatively larger lanthanoid(II) ions, and we report structures of [Eu₂(Odpp)(μ-Odpp)₃] (**1**), Yb₂(Odpp)₂(μ-Odpp)₂ (**2**) and the intriguing mixed-valent homoleptic aryloxide [Yb₃(Odpp)₇] (**3**). In addition, a novel synthesis of the homoleptic complexes by direct reaction of the lanthanoid metals with the phenol at elevated temperatures is presented.

Results and Discussion

Syntheses and characterisation: The lanthanoid(II) aryloxides [Ln(Odpp)₂] (Ln = Eu, Yb) were prepared by heating a mixture of the metal, mercury and 2,6-diphenylphenol (HOdpp) to 200 °C in an evacuated and sealed Carius tube [Eq. (1)]. These reactions were performed in the absence of



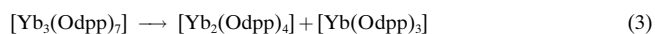
any added solvent, although initially the molten HOdpp (m.p. 100–102 °C) possibly acted in this capacity. In the absence of mercury, Yb metal and HOdpp react only incompletely at 350 °C after 6 days. Mercury presumably activates the metal surface by amalgamation and may also contribute through slight dissolution in the molten phenol, since the metal has significant solubility in organic solvents.^[6] There have been a number of conceptually related reactions of lanthanoid metals with low acidity protic reagents: for example, i) metal-atom reactions with primary acetylenes^[1a,b,d] and pentamethylcyclopentadiene,^[1a,b,d] ii) reaction of mercury-activated lanthanoids with alcohols,^[1g,j] (where oxoalkoxide cages [Ln₅O-(iPrO)₁₃] can be formed^[1g,j] from isopropyl alcohol), iii) coordination-assisted direct reaction of 2-methoxyethanol with metals,^[1j, 7] and iv) reaction of Yb or Eu with cyclopentadiene^[1a,b,d] or bulky 2,6-disubstituted phenols^[7, 8] in liquid ammonia, *N*-methylimidazole or acetonitrile. However, the present reactions are particularly simple and deliver homoleptic complexes from bulk metals in the absence of any donor solvent and without coordination of the phenol (cf. isolation of alcohol solvates from Ln/ROH reactions^[1g,j]). There is considerable potential for analogous reactions with other protic reagents including amines, phosphines and thiols.

Extraction of the reaction mixtures with toluene followed by crystallisation yielded [Eu₂(Odpp)₄](PhMe) (**1**·(PhMe)) and [Yb₂(Odpp)₄](PhMe)_{1.5} (**2**·(PhMe)_{1.5}). The yield of **2**·(PhMe)_{1.5} was low even after exhaustive extraction of the reaction residue with hot toluene, and much red-orange toluene-insoluble solid remained mixed with the excess of Yb(Hg). When this material was kept in a small amount of toluene for ≈2 months, some orange-red crystals were collected and identified by X-ray crystallography as the

mixed-valent species [Yb₃(Odpp)₇](PhMe) (**3**·PhMe) [Eq. (2)].



From a separate preparation of the mixture of **2** and **3**, the toluene-insoluble residue (i.e. free of **2**) was extracted with PhMe/THF. Evaporation to dryness and fractional crystallisation of the residue from toluene yielded successively **2**·(PhMe)_{1.5} and then the known [Yb(Odpp)₃].^[4a] Thus, THF induced dissociation of the mixed valence **3** [Eq. (3)].



Initially, the known [Yb(Odpp)₂(thf)₃]^[9] and [Yb(Odpp)₃(thf)₂]^[4a] would presumably have been formed by THF treatment, but these were evidently desolvated on workup with toluene. It is apparent that **2** and [Yb(Odpp)₃] do not reform **3** in boiling toluene, hence the thermal synthesis [Eq. (2)] is a unique source of this species. No species analogous to **3** was observed in the reaction with europium, consistent with the greater stability of Eu^{II} than Yb^{II}.^[1c,d]

Complexes **1**·(PhMe) and **2**·(PhMe)_{1.5} gave satisfactory elemental analyses and their infrared spectra showed absorptions characteristic of the Odpp ligand. There were some differences between the spectra of **1** and **2** consistent with their different structures. No metal-containing ions were detected in the EI mass spectra of **1** and **2**, in contrast to the observation of ions attributable to [Yb(Odpp)₂]⁺ and [Yb(Odpp)]⁺ in the spectrum of [Yb(Odpp)₂(thf)₃].^[9] This is presumably due to the less volatile nature of binuclear **1** and **2** than monomeric [Yb(Odpp)₂(thf)₃].

The ¹⁷¹Yb chemical shift of diamagnetic **2** in toluene is close to that (δ = 314) of [{Yb(OC₆H₂-2,6-*t*Bu-4-Me)₂}]₂ in the same solvent,^[5b] consistent with persistence of the dimeric structure in solution. The ¹H NMR spectrum in [D₆]benzene showed a complex series of overlapping resonances for the Odpp ligands and the toluene of crystallisation. However, a distinct doublet of doublets at δ = 7.38, which integrated for 16H, can be assigned to the *ortho* protons of the substituent phenyl groups. This implies a single Odpp environment, in contrast to the observation of separate bridging and terminal aryloxide resonances in the spectrum of dimeric [{Yb(OC₆H₂-2,6-*t*Bu-4-Me)₂}]₂.^[5] Therefore, the spectrum of **2** probably results from rapid exchange of Odpp ligands, which are less bulky than 2,6-di-*tert*-butyl-4-methylphenolate groups. Further, the C₂ symmetry of the Odpp resonances in solution suggests loss of the unsymmetrical intramolecular Yb–(Odpp) π-arene coordination observed in the solid state (see below), possibly owing to Yb–C₆D₆ interactions. Unfortunately, **2** crystallised from solution at lower temperatures, precluding variable-temperature studies. In [D₈]THF, the spectrum of **2** showed more distinct resonances than in [D₆]benzene, but it presumably corresponds to a [D₈]THF complex analogous to the reported [Yb(Odpp)₂(thf)₃].^[9] Integration of the toluene resonances in the spectrum in [D₈]THF was consistent with the composition established by microanalysis and X-ray crystallography (see below). The

separation and spectroscopic characterisation of the mixed-valent complex **3** were prevented by its low solubility in noncoordinating solvents. The ^1H NMR spectrum of the bulk material in $[\text{D}_8]\text{THF}$ was consistent with an approximately 2:1 mixture of $[\text{Yb}(\text{Odpp})_2]$ and $[\text{Yb}(\text{Odpp})_3]$. The resonances of the latter were severely shifted and broadened due to the paramagnetism of Yb^{III} and were separate from those of diamagnetic $[\text{Yb}(\text{Odpp})_2]$. The $[\text{D}_8]\text{THF}$ -induced dissociation of **3** is consistent with the behaviour on THF/toluene extraction [Eq. (3)].

Crystal structure analyses: The structures of **1–3** are displayed in Figures 1–3, whilst selected bond lengths and angles are given in Tables 1–3. Compound **1** has an unsymmetrical binuclear structure (Figure 1) in which Eu(1) has one terminal

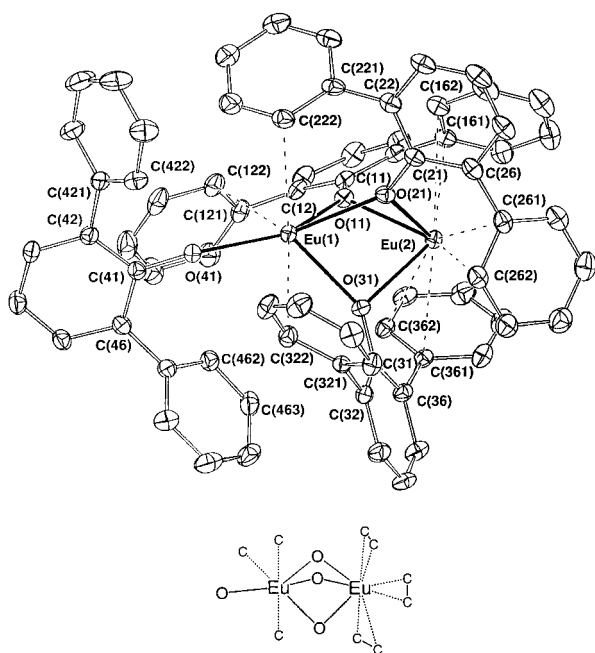


Figure 1. a) Molecular projection of $[\text{Eu}_2(\text{Odpp})_4]$ (**1**) normal to the $\text{Eu}(1)\text{--Eu}(2)$ axis with 20% thermal ellipsoids; b) simplified representation showing the donor atoms. Partially coordinated (η^1 or η^2) phenyl rings are shown by single atoms or ring fragments.

and three bridging Odpp ligands, and Eu(2) only three bridging Odpp ligands. Oxygen ligation leaves gaps in the coordination sphere, especially at Eu(2), and these are filled by π -phenyl–europium interactions (see below). The structure has the same unusual $(\text{ArO})\text{Eu}(\mu\text{-OAr})_3\text{Eu}$ framework as in the recently reported $[\text{Eu}_2(\text{OC}_6\text{H}_3\text{Me}_2\text{-}2,6)_4(\text{dme})_3]$ ($\text{dme} = 1,2\text{-dimethoxyethane}$), where one Eu has a terminal and three bridging OAr groups and one chelating dme, whilst the other has three bridging OAr groups and two chelating dme ligands.^[10] Accordingly, in **1** the intramolecular $\pi\text{-Ph}\text{--Eu}$ interactions, combined with the steric bulk of the phenyl substituents, effectively replace one dme at Eu(1) and two dme ligands at Eu(2). Furthermore, the $\text{Eu}\text{--O}$ bond lengths in **1** (Table 1) are comparable with $\text{Eu}\text{--OAr}$ distances of aryloxeuropium(II) complexes with formal coordination numbers ≥ 5 , for example $[\text{Eu}(\text{OC}_6\text{H}_2\text{-}2,6\text{-}t\text{Bu}_2\text{-}4\text{-}$

Table 1. Selected geometries for $[\text{Eu}_2(\text{Odpp})_4] \cdot (\text{toluene})$, **1**·(PhMe) (distances in Å, angles in $^\circ$).

$\text{Eu}(1)\text{--O}(11)$	2.493(2)	$\text{Eu}(2)\text{--O}(11)$	2.463(3)
$\text{Eu}(1)\text{--O}(21)$	2.517(3)	$\text{Eu}(2)\text{--O}(21)$	2.426(3)
$\text{Eu}(1)\text{--O}(31)$	2.428(2)	$\text{Eu}(2)\text{--O}(31)$	2.438(2)
$\text{Eu}(1)\text{--O}(41)$	2.361(3)		
$\text{Eu}(1)\cdots\text{C}(122)$	3.222(5)	$\text{Eu}(2)\cdots\text{C}(161)$	2.987(4)
$\text{Eu}(1)\cdots\text{C}(222)$	3.082(4)	$\text{Eu}(2)\cdots\text{C}(162)$	3.154(4)
$\text{Eu}(1)\cdots\text{C}(322)$	3.240(4)	$\text{Eu}(2)\cdots\text{C}(261)$	3.036(4)
		$\text{Eu}(2)\cdots\text{C}(262)$	3.013(4)
		$\text{Eu}(2)\cdots\text{C}(361)$	3.043(4)
		$\text{Eu}(2)\cdots\text{C}(362)$	3.136(4)
$\text{Eu}(1)\cdots\text{Eu}(2)$	3.534(1)		
$\text{O}(11)\text{--Eu}(1)\text{--O}(21)$	71.45(8)	$\text{O}(11)\text{--Eu}(2)\text{--O}(21)$	73.50(9)
$\text{O}(11)\text{--Eu}(1)\text{--O}(31)$	77.57(8)	$\text{O}(11)\text{--Eu}(2)\text{--O}(31)$	77.95(8)
$\text{O}(21)\text{--Eu}(1)\text{--O}(31)$	71.10(8)	$\text{O}(21)\text{--Eu}(2)\text{--O}(31)$	72.49(8)
$\text{O}(11)\text{--Eu}(1)\text{--O}(41)$	143.45(8)	$\text{Eu}(1)\text{--O}(11)\text{--Eu}(2)$	90.96(8)
$\text{O}(21)\text{--Eu}(1)\text{--O}(41)$	140.52(8)	$\text{Eu}(1)\text{--O}(21)\text{--Eu}(2)$	91.24(9)
$\text{O}(31)\text{--Eu}(1)\text{--O}(41)$	123.08(8)	$\text{Eu}(1)\text{--O}(31)\text{--Eu}(2)$	93.15(8)
$\text{Eu}(1)\text{--O}(11)\text{--C}(11)$	150.0(2)	$\text{Eu}(2)\text{--O}(11)\text{--C}(11)$	116.9(2)
$\text{Eu}(1)\text{--O}(21)\text{--C}(21)$	148.5(2)	$\text{Eu}(2)\text{--O}(21)\text{--C}(21)$	118.5(2)
$\text{Eu}(1)\text{--O}(31)\text{--C}(31)$	147.2(2)	$\text{Eu}(2)\text{--O}(31)\text{--C}(31)$	119.6(2)
$\text{Eu}(1)\text{--O}(41)\text{--C}(41)$	154.6(2)		

$\text{Me}_2(\text{thf})_3]$ ^[11] ($\text{CN} = 5$; $\text{Eu}\text{--O}_{\text{ter}}$ 2.321(5), 2.337(5) Å), $[\text{Eu}(\text{OC}_6\text{H}_3\text{-}2,6\text{-Me}_2)_2(\text{CH}_3\text{CN})_4]$ ^[8b] ($\text{CN} = 6$; $\text{Eu}\text{--O}_{\text{ter}}$ 2.313(12), 2.35(2) Å), $[\text{Eu}_2(\text{OC}_6\text{H}_3\text{-}2,6\text{-Me}_2)_4(\text{dme})_3]$ ^[10] ($\text{CN} = 6$; $\text{Eu}\text{--O}_{\text{ter}}$ 2.350(5); $\text{Eu}\text{--O}_{\text{br}}$ 2.477(6)–2.597(5) Å) ($\text{CN} = 7$; $\text{Eu}\text{--O}_{\text{br}}$ 2.447(5)–2.495(5) Å).^[10] Thus, the $\pi\text{-Ph}\text{--Eu}$ coordination lengthens the $\text{Eu}\text{--O}$ distances. For Eu(1), intramolecular $\pi\text{-Ph}\text{--Eu}$ coordination comprises three $\eta^1\text{-Ph}\text{--Eu}$ contacts whilst for Eu(2) there are three $\eta^2\text{-Ph}\text{--Eu}$ interactions. The $\text{Eu}\text{--C}$ distances that are considered to represent significant $\pi\text{-Ph}\text{--Eu}$ interactions lie in the range 2.987(4) to 3.240(4) Å (av. 3.11 Å) (Table 1). For the dimer $[[\text{Nd}(\text{OAr})_2(\mu\text{-}\{O:\eta^6\text{-Ar}\}\text{-OAr})_2]]$ ($\text{Ar} = 2,6\text{-}i\text{Pr}_2\text{C}_6\text{H}_3$), which has $\pi\text{-}\eta^6\text{-Ar}\text{--Nd}$ bonding linking the $\text{Nd}(\text{OAr})_3$ units, the $\text{Nd}\text{--C}$ bonds span 2.898(12) to 3.183(10) Å (av. 3.03 Å).^[3a] Allowing for the larger size of Eu^{2+} than Nd^{3+} (difference 0.15 Å),^[12] these ranges are similar or even suggest stronger bonding to Eu^{II} . They are entirely consistent with $\text{Ln}\text{--C}$ distances in complexes of Ln metals with neutral π donors,^[13] such as $[[\text{Eu}(\eta^6\text{-C}_6\text{Me}_6)(\text{AlCl}_4)_2]_4]$ ($\text{Eu}\text{--C}$ 3.00 Å; the angle brackets denote an average value).^[13c] Given that virtually half of the coordination sphere of Eu(2) is available for $\pi\text{-Ph}\text{--Eu}$ bonding, the number of interacting carbons seems small, but is presumably affected by the combined steric effect of the three interacting rings. The next shortest $\text{Eu}(2)\text{--C}$ distance ($\text{Eu}(2)\text{--C}(366)$ 3.319(5) Å) is near the binding limit and might reasonably be considered, but it has been excluded as it is ≈ 0.15 Å more distant than the next closest carbon to Eu(2). There is no interaction between the toluene of crystallisation and the metals.

Surprisingly, the structure of **1** bears a striking resemblance to that of the homoleptic anionic 2,6-diphenylphenolato-neodymium(III) complex $[\text{Na}\{\text{Nd}(\text{Odpp})_4\}]^{\text{[14]}}$ which contains a $[\text{Nd}(\text{Odpp})_4]^-$ anion and an aryloxo-bridged and phenyl-encapsulated Na^+ cation. This suggests that **1** may be described similarly (i.e. a $[\text{Eu}(\text{Odpp})_4]^{2-}$ dianion coordinated to an Eu^{2+} dication). As with Nd in $[\text{Na}\{\text{Nd}(\text{Odpp})_4\}]$, the geometry at Eu(1) in **1** is highly distorted from tetrahedral by virtue of the bridging of three oxygens to the second metal

centre (in this case Eu(2)). This is indicated by the small $O_{br}-Eu(1)-O_{br}$ and large $O_{ter}-Eu(1)-O_{br}$ angles (Table 1), whereas discrete $[Ln(Odpp)_4]^-$ anions have a more regular geometry^[14b] (see also below). The three bridging Odpp ligands are inclined toward Eu(2) with $Eu(1)-O(n1)-C(n1)$ ($n=1-3$) angles significantly larger than the corresponding angles at Eu(2) and only marginally smaller than $Eu(1)-O(41)-C(41)$ of the terminal Odpp in **1** (Table 1).

The crystal structure of **2** showed two crystallographically independent but closely similar dimeric molecules (i and ii). Pseudosymmetry is evident, and the possibility that the crystal symmetry assignment as triclinic rather than monoclinic may be a consequence of poor crystal quality cannot be totally discarded. Nevertheless, at a low level of precision the nature of the material is definitively established, as shown by the typical **2(i)** in Figure 2. Toluene of crystallisation (1.5 molecules per dimer) was also present in the unit cell. The complex is approximately symmetrical with two bridging and two terminal Odpp ligands around each ytterbium. However, the structure differs strikingly from that of solvent-free, dimeric $[[Yb(OC_6H_2-2,6-tBu_2-4-Me)_2]_2]^{[5]}$ since there is approximately pyramidal YbO_3 geometry in **2(i)** (Σ_{O-Yb-O} 261.6, 276.9°) compared with near-trigonal planar in $[[Yb(OC_6H_2-2,6-tBu_2-4-Me)_2]_2]^{[5]}$ (Σ_{O-Yb-O} 352.1, 359.9°).^[5] The $Yb(\mu-OAr)_2Yb$ geometry is similar in both complexes ($Yb-O_{br}-Yb$ 100.1(7) to 107.8(7)° and $O_{br}-Yb-O_{br}$ 72.6(6) to 80.6(6)° in the two structures), but in **2(i)** the terminal $Yb-OAr$ bonds form angles of 96.5 and 104.6° to the $Yb-Yb$ vector, by contrast with 161.2 and 165.7° in $[[Yb(OC_6H_2-2,6-tBu_2-4-Me)_2]_2]^{[5]}$. The resulting void in the coordination sphere on each ytterbium atom in **2(i)** is filled by a number of close ytterbium-carbon(phenyl) contacts (below). The $Yb-O$ distances (Table 2) are comparable with those of $[[Yb(OC_6H_2-2,6-tBu_2-4-Me)_2]_2]^{[5]}$ ($Yb-O_{ter}$ 2.08(2), 2.10(2); $Yb-O_{br}$ 2.25(2)–2.37(2) Å).^[5] The $Yb-C$ distances considered (from data in ref. [13]) to be π -Ph- Yb interactions lie in the range 2.75(3) to 3.18(4) Å (Table 2). The shortest of these is similar to those of a $Yb^{II}-\eta^2$ -olefin complex, namely $[Yb(C_5Me_5)_2(\mu-\eta^2:\eta^2-CH_2CH_2)-$

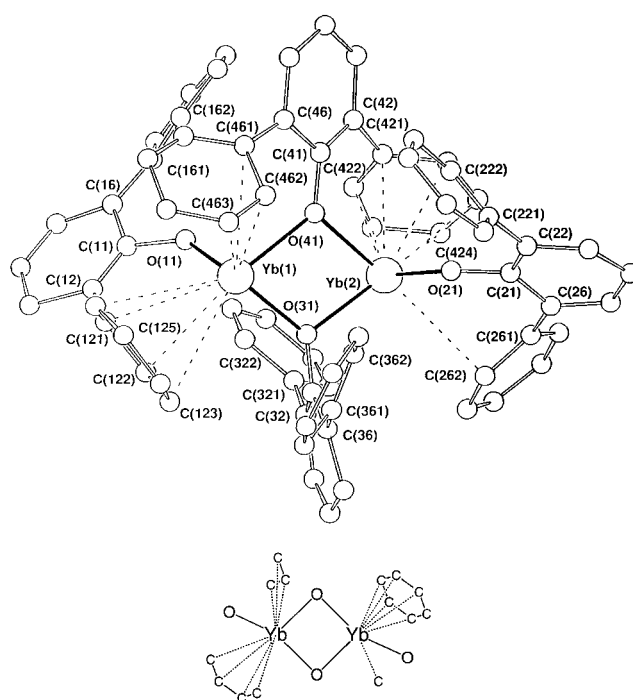


Figure 2. a) Molecular projection of molecule **i** of $[Yb_2(Odpp)_4]$ (**2(i)**) normal to the Yb_2O_2 plane with 20% thermal envelopes; b) simplified representation showing the donor atoms. Partially coordinated (η^1 , η^3 , or η^4) phenyl rings are shown by single atoms or ring fragments.

$PtMe_2]$, $Yb-C$ 2.781 ± 0.006 Å^[15] and the range of proposed $Yb^{II}-C$ interactions is similar to $Nd-C$ (2.898(12) to 3.183(10) Å) of $[[Nd(OAr)_2(\mu-O:\eta^6-Ar)-OAr]_2]$ ($Ar=2,6-iPr_2C_6H_3$).^[3a] For the same coordination number, the ionic radius of Yb^{2+} is approximately 0.04 Å larger than that of Nd^{3+} .^[12] For **2(i)**, the intramolecular π -Ph- Yb bonding can be described as one η^3 -Ph (C(1461–1463)) and one η^4 -Ph (C(1121–1123,1126)) at $Yb(11)$ and as one η^6 -Ph (C(1421–1426)) and one η^1 -Ph (C(1262)) at $Yb(12)$. An $Yb-ipsoc$ contact ($Yb(12)-C(131)$ 3.10(7) Å) is also close enough to be viewed as bonding but is considered to result more from the

Table 2. Selected geometries for $[Yb_2(Odpp)_4] \cdot (toluene)_{1.5} \cdot 2 \cdot (PhMe)_{1.5}$ (distances in Å, angles in °). The two values in each entry are for molecules $n=i, ii$.^[a]

	i	ii		i	ii
$Yb(n1)-O(n11)$	2.10(2)	2.11(2)	$Yb(n2)-O(n21)$	2.17(2)	2.14(2)
$Yb(n1)-O(n31)$	2.30(2)	2.29(2)	$Yb(n2)-O(n31)$	2.24(2)	2.34(2)
$Yb(n1)-O(n41)$	2.32(2)	2.35(2)	$Yb(n2)-O(n41)$	2.30(2)	2.31(2)
$Yb(n1) \cdots C(n121)$	3.09(4)	3.13(3)	$Yb(n2) \cdots C(n262)$	3.18(4)	3.18(4)
$Yb(n1) \cdots C(n122)$	3.01(3)	3.09(3)	$Yb(n2) \cdots C(n421)$	2.82(3)	2.88(3)
$Yb(n1) \cdots C(n123)$	3.19(4)	3.28(4)	$Yb(n2) \cdots C(n422)$	2.80(4)	2.75(3)
$Yb(n1) \cdots C(n126)$	3.23(5)	3.29(4)	$Yb(n2) \cdots C(n423)$	2.85(4)	3.07(4)
$Yb(n1) \cdots C(n461)$	3.11(4)	2.96(3)	$Yb(n2) \cdots C(n424)$	3.08(4)	3.10(4)
$Yb(n1) \cdots C(n462)$	2.86(3)	2.86(4)	$Yb(n2) \cdots C(n425)$	3.18(4)	3.12(4)
$Yb(n1) \cdots C(n463)$	3.22(4)	3.27(4)	$Yb(n2) \cdots C(n426)$	2.99(4)	2.93(4)
$Yb(n1) \cdots Yb(n2)$	3.675(3)	3.682(3)			
$O(n11)-Yb(n1)-O(n31)$	103.4(8)	109.3(8)	$O(n21)-Yb(n2)-O(n31)$	108.6(7)	102.1(8)
$O(n11)-Yb(n1)-O(n41)$	85.6(8)	92.3(8)	$O(n21)-Yb(n2)-O(n41)$	95.8(8)	93.3(8)
$O(n31)-Yb(n1)-O(n41)$	72.6(6)	75.3(7)	$O(n31)-Yb(n2)-O(n41)$	74.1(6)	75.0(7)
$Yb(n1)-O(n31)-Yb(n2)$	107.8(7)	105.4(8)	$Yb(n1)-O(n41)-Yb(n2)$	105.5(7)	104.3(7)
$Yb(n1)-O(n31)-C(n31)$	134(2)	138(2)	$Yb(n1)-O(n41)-C(n41)$	131(2)	128(2)
$Yb(n2)-O(n31)-C(n31)$	118(2)	115(2)	$Yb(n2)-O(n41)-C(n41)$	124(2)	128(2)

[a] Angles at $O(n11:n21)$ are 139(2), 144(2); 145(2), 145(2)°. Dihedral angles between the C_6 planes of rings $C(n3m; n4m)$ to their central Yb_2O_2 planes are 75.8(9), 72.2(8); 24.4(8), 18.8(8)°. $O(n31) \cdots O(n41)$ are 2.74(3), 2.83(3) Å.

arrangement of the bridging aryloxy than formation of a discrete Yb–C bond. In a comparison of **2(i)** as typical with $[\text{Nd}(\text{Odpp})_3]^{[4a]}$ which has η^6 - and η^1 -Ph interactions, the $\langle \text{Yb}(12)\text{--C} \rangle$ distance for the η^6 -Ph–Yb(12) interaction (2.9₅ Å; the subscripted number is of less reliable accuracy) is similar to $\langle \text{Nd--C} \rangle$ (3.04₆ Å) of the η^6 -bonded ring. This is the more significant given the slightly larger radius of Yb^{2+} (above).^[12] It is also relevant that the $\langle \text{Yb--C} \rangle$ distance of the η^6 -Ph ring in **2(i)** is comparable with $\langle \text{Yb--C} \rangle$ (2.97₈ Å) of η^6 -Ph–Yb of $[\text{Yb}(\text{Odpp})_3]^{[4a]}$ (isostructural with $[\text{Nd}(\text{Odpp})_3]$) even though Yb^{3+} is approximately 0.15 Å smaller than Yb^{2+} .^[12] This further emphasises the importance of intramolecular π -Ph–Yb interactions in **2**. However, the η^1 -Ph–Yb contact (Table 2) is longer than η^1 -Ph–Nd (2.964(7) Å) of $[\text{Nd}(\text{Odpp})_3]^{[4a]}$. The Yb(12)–cent(146) vector (cent(146) = centroid of atoms C(1421–1426)) is nearly perpendicular to the phenyl ring plane (θ defined as the angle between the normal to the η^6 -phenyl plane and the Yb–cent(146) vector, $\theta = 8.6^\circ$) and the Yb(12)–cent(146) distance is 2.6₁ Å. The phenyl interactions at Yb(11) appear longer than those at Yb(12) with $\langle \text{Yb}(11)\text{--C} \rangle$ 3.1₄ Å (η^4 -Ph) and 3.0₆ Å (η^3 -Ph). The next shortest contacts (C(1124) 3.32(4) Å; C(1125) 3.32(5) Å) are seemingly too distant for π -bonding. However, the angle θ between the normal of the plane defined by C(1121–1126) and the Yb(11)–cent(116) vector is 7.8°, marginally smaller than that of the η^6 -Ph bound to Yb(12). This suggests that the ring C(1121–1126) may also be described as η^6 -Ph-bound, albeit more weakly, since the Yb(11)–cent(116) distance (2.8₈ Å) is considerably longer than Yb(12)–cent(146) (see above). The structure of dimer **2(ii)** (Table 2) is similar to that of dimer **2(i)**.

The structure of **3** revealed an ionic mixed-valent complex containing discrete $[\text{Yb}_2^{\text{II}}(\text{Odpp})_3]^+$ cations and $[\text{Yb}^{\text{III}}(\text{Odpp})_4]^-$ anions (Figure 3). The $[\text{Yb}_2(\text{Odpp})_3]^+$ cation is a structure unique amongst lanthanoid aryloxides since it has no terminal aryloxy groups. Three Odpp ligands bridge the two ytterbium centres, and the naked faces of the metals are surrounded by pendant phenyl groups. The decrease in size from Eu^{2+} to Yb^{2+} results in loss of a terminal Odpp group between **1** and $[\text{Yb}_2(\text{Odpp})_3]^+$. The range of Yb–O distances (2.289(7)–2.327(7) Å Table 3) is close to those observed for the bridging Odpp ligands in **2** (see above), indicative of oxidation state (II) for ytterbium, whilst the O–Yb–O angles (70.3(2)–75.6(2)°, Table 4) are similar to the $\text{O}_{\text{br}}\text{--Eu--O}_{\text{br}}$ angles in **1** (Table 1). The geometry of the oxygens of the bridging Odpp ligands is characterised by much narrower Yb–O–Yb angles compared with **2**, leading to a closer nonbonded Yb–Yb separation (3.348 Å c.f. **2(i)** 3.675 Å) and this can be attributed to the extra bridging Odpp in $[\text{Yb}_2(\text{Odpp})_3]^+$. In contrast to those of **1**, the Ln–O–C angles in the cation of **3** (Table 3) do not show a marked variation, reflecting the more symmetrical nature of the Yb(μ -Odpp)₃–Yb framework. The primary coordination of the ytterbium centres in $[\text{Yb}_2(\text{Odpp})_3]^+$ is augmented by π -phenyl–ytterbium interactions. An η^6 -Ph–Yb and two η^1 -Ph–Yb groups are observed for Yb(2) and an η^6 -Ph–Yb, an η^2 -Ph–Yb and an η^1 -Ph–Yb for Yb(3) (Table 3). The $\langle \text{Yb}(2)\text{--C}(103\text{--}108) \rangle$ 3.03₇ Å and $\langle \text{Yb}(3)\text{--C}(85\text{--}90) \rangle$ 2.96₈ Å for the η^6 -phenyls are in agreement with values for **2** (above) and are comparable with

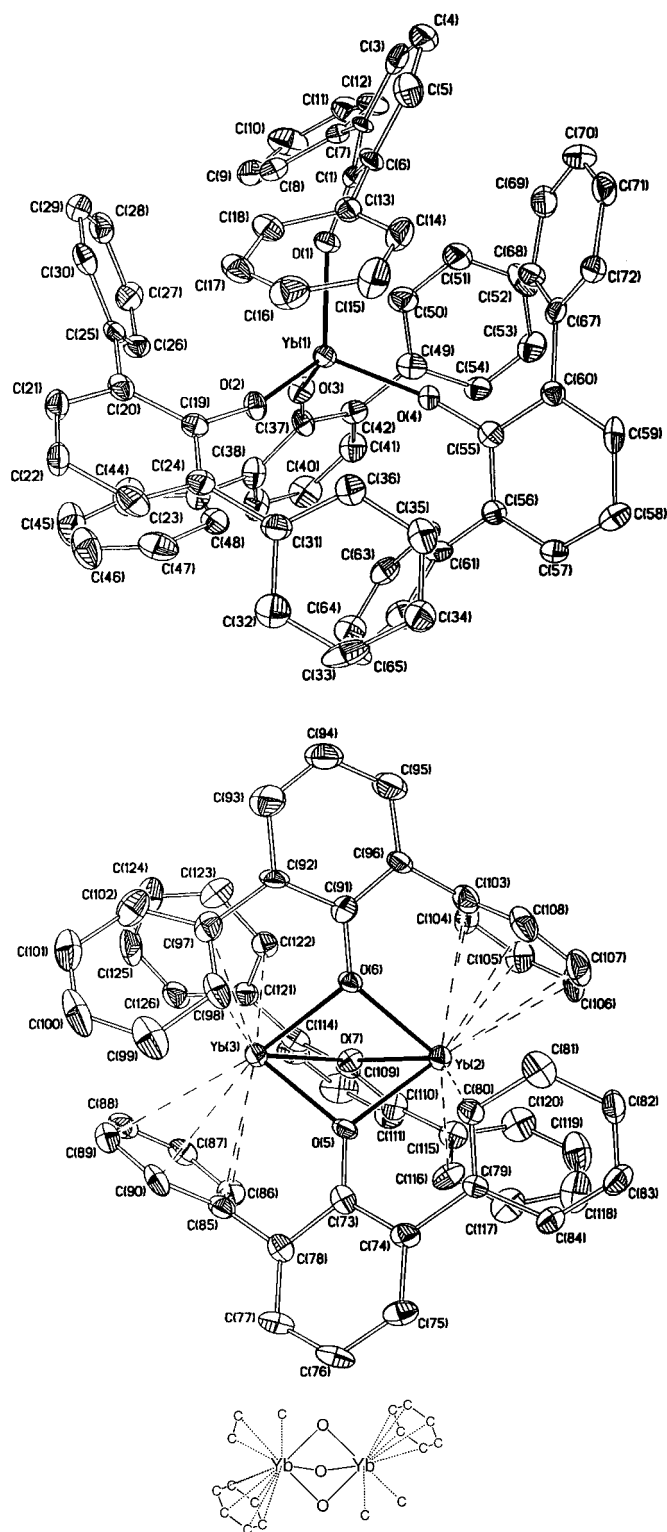


Figure 3. Structure of $[\text{Yb}_2(\text{Odpp})_3]^+[\text{Yb}(\text{Odpp})_4]^-$ (**3**). a) The $[\text{Yb}(\text{Odpp})_4]^-$ anion; b) the $[\text{Yb}_2(\text{Odpp})_3]^+$ cation projected normal to the Yb(2)–Yb(3) axis with 30% thermal ellipsoids; c) simplified representation showing the donor atoms. Partially coordinated (η^1 or η^2) phenyl rings are shown by single atoms or ring fragments.

Eu--C values for **1** allowing for ionic radii differences,^[12] whilst the Yb–centroid vectors are nearly perpendicular to the phenyl ring planes (Yb(2)–C(103–108), $\theta = 4.7^\circ$; Yb(3)–C(85–90), $\theta = 5.2^\circ$), indicative of η^6 bonding. The remaining

Table 3. Selected geometries for $[\text{Yb}(\text{Odpp})_4][\text{Yb}_2(\text{Odpp})_3] \cdot (\text{toluene})$, **3**·(PhMe) (distances in Å, angles in °).

Yb(1)–O(1)	2.094(7)	Yb(2)–O(5)	2.320(7)
Yb(1)–O(2)	2.049(7)	Yb(2)–O(6)	2.289(7)
Yb(1)–O(3)	2.073(8)	Yb(2)–O(7)	2.302(7)
Yb(1)–O(4)	2.053(6)	Yb(3)–O(5)	2.313(7)
		Yb(3)–O(6)	2.319(6)
		Yb(3)–O(7)	2.327(7)
Yb(2)···C(80)	3.06(1)	Yb(3)···C(85)	2.87(1)
Yb(2)···C(103)	2.99(1)	Yb(3)···C(86)	2.88(1)
Yb(2)···C(104)	3.04(1)	Yb(3)···C(87)	2.97(1)
Yb(2)···C(105)	3.15(1)	Yb(3)···C(88)	3.06(1)
Yb(2)···C(106)	3.10(1)	Yb(3)···C(89)	3.06(1)
Yb(2)···C(107)	3.00(1)	Yb(3)···C(90)	2.97(1)
Yb(2)···C(108)	2.94(1)	Yb(3)···C(97)	3.12(1)
Yb(2)···C(116)	2.85(1)	Yb(3)···C(98)	2.97(1)
		Yb(3)···C(122)	3.04(1)
Yb(2)···Yb(3)	3.3480(6)		
O(1)–Yb(1)–O(2)	114.9(3)	O(6)–Yb(2)–O(7)	75.6(2)
O(1)–Yb(1)–O(3)	109.9(3)	O(5)–Yb(3)–O(6)	70.3(2)
O(1)–Yb(1)–O(4)	111.0(3)	O(5)–Yb(3)–O(7)	74.1(2)
O(2)–Yb(1)–O(3)	112.1(3)	O(6)–Yb(3)–O(7)	74.6(2)
O(2)–Yb(1)–O(4)	106.5(3)	Yb(2)–O(5)–Yb(3)	92.5(3)
O(3)–Yb(1)–O(4)	101.6(3)	Yb(2)–O(6)–Yb(3)	93.2(3)
Yb(1)–O(1)–C(1)	154.8(7)	Yb(2)–O(7)–Yb(3)	92.6(3)
Yb(1)–O(2)–C(19)	165.7(7)	Yb(2)–O(5)–C(73)	131.5(7)
Yb(1)–O(3)–C(37)	162.5(7)	Yb(3)–O(5)–C(73)	132.5(6)
Yb(1)–O(4)–C(55)	164.3(6)	Yb(2)–O(6)–C(91)	135.4(6)
O(5)–Yb(2)–O(6)	70.7(3)	Yb(3)–O(6)–C(91)	123.4(6)
O(5)–Yb(2)–O(7)	74.5(2)	Yb(2)–O(7)–C(109)	136.7(6)
		Yb(3)–O(7)–C(109)	130.5(6)

Table 4. Ln···C contacts considered to be significant interactions in **1**, **2**, the cation of **3**, and related lanthanoid complexes with neutral π -donor ligands.

Complex	Ln···C [Å]	$\langle \text{Ln} \cdots \text{C} \rangle$ [Å]	Ref.
1	2.987(4)–3.240(4)	3.11	
2	2.75(3)–3.18(4)	3.00	
$[\text{Yb}_2(\text{Odpp})_3]^+$ in 3	2.85(1)–3.15(1)	3.00	
$[\{\text{Nd}(\text{OAr})_2(\mu\text{-}\{\text{O}:\eta^6\text{-Ar}\}\text{-OAr})_2\}]$	2.898(12)–3.183(10)	3.03	[3a]
$[\{\text{Eu}(\eta^6\text{-C}_6\text{Me}_6)(\text{AlCl}_4)_2\}_2]$	2.917(15)–3.066(12)	3.00	[13c]
$[\text{Yb}(\text{C}_5\text{Me}_5)_2(\mu\text{-}\eta^2\text{-}\eta^2\text{-C}_2\text{H}_4)\text{PtMe}_2]$	2.781 ± 0.006		[15]
$[\text{Nd}(\text{Odpp})_3]$	2.946(6)–3.158(9)	3.03	[4b]
$[\text{Yb}(\text{Odpp})_3]$	2.814(4)–3.148(6)	2.96	[4a]

close Yb–C distances lie in the range 2.85(1)–3.12(1) Å and correspond well with Yb–C (2.75(3)–3.18(4)) of **2**. Moreover, the present range for Yb^{II}–C bonds (2.85(1)–3.15(1) Å) is close to that (2.814(4)–3.148(6) Å) for Yb^{III}–C interactions for the π - η^6 -Ph and π - η^1 -Ph groups of $[\text{Yb}(\text{Odpp})_3]$,^[4a] despite the much larger size of Yb²⁺. A summary of Ln–C interactions of **1**, **2**, the cation of **3**, and of relevant comparable compounds is given in Table 4.

The ytterbium of the discrete $[\text{Yb}(\text{Odpp})_4]^-$ anion in **3** lies in an only slightly distorted tetrahedral metal environment as indicated by O–Yb–O angles close to 109° (Table 3). The range of angles compares well with those observed for the anions in $[\text{Na}(\text{diglyme})_2][\text{Ln}(\text{Odpp})_4]$ (Ln = Nd or Er) (O–Ln–O 101.7(1)–115.4(1)° (Nd), 102.9(2)–112.7(2)° (Er)).^[14] In addition, the $\langle \text{Yb}–\text{O} \rangle$ distance (2.06₅ Å) is smaller than the corresponding $\langle \text{Nd}–\text{O} \rangle$ (2.18₇ Å) and $\langle \text{Er}–\text{O} \rangle$ (2.08₂ Å) distances, which correlates with differences in the ionic radii of the Ln³⁺ ions (i.e. Yb³⁺ is approximately 0.11 Å smaller than Nd³⁺ and 0.02 Å smaller than Er³⁺).^[12] Since the ionic

radius of Yb²⁺ is approximately 0.13 Å larger than Yb³⁺,^[12] the above distances unambiguously define the ytterbium in the anion as trivalent. Interestingly, $\langle \text{Yb}–\text{O} \rangle$ is near-identical with that (2.06₅ Å) of Yb(Odpp)₃ (with η^6 - π -Ph and η^1 - π -Ph).^[4a]

Structurally characterised organometallic compounds combining lanthanoids in both the II and III oxidation states are very rare, specifically, $[\{\text{Yb}^{\text{III}}(\text{C}_5\text{Me}_5)_2\}_2\text{Yb}^{\text{II}}(\mu\text{-CCPh})_4]$,^[16] $[\text{Sm}^{\text{III}}(\text{C}_5\text{Me}_5)_2(\mu\text{-C}_5\text{H}_5)\text{Sm}^{\text{II}}(\text{C}_5\text{Me}_5)_2]$,^[17] $[\{\text{Yb}^{\text{III}}(\text{C}_5\text{Me}_5)_2(\mu\text{-F})_2\text{Yb}^{\text{II}}(\text{C}_5\text{Me}_5)_2\}]$,^[18] $[\text{Yb}^{\text{III}}(\text{C}_5\text{Me}_5)_2(\mu\text{-F})\text{Yb}^{\text{II}}(\text{C}_5\text{Me}_5)_2]$,^[19] and $[\text{Yb}^{\text{III}}\text{Ph}_2(\text{thf})(\mu\text{-Ph})_3\text{Yb}^{\text{II}}(\text{thf})_3]$.^[20] Compound **3** is the first mixed oxidation state aryloxide and further novelty is provided by the ionic constitution.

Conclusion

The homoleptic lanthanoid(II) 2,6-diphenylphenolates **1**, **2**, and $[\text{Yb}_2(\text{Odpp})_3]^+$ are unique complexes showing the versatility of the phenyl substituents in occupying considerable sectors of the lanthanoid coordination sphere and influencing the geometries of the lanthanoid–oxygen framework.

Experimental Section

General: The compounds described herein are extremely air- and moisture-sensitive and consequently all operations were carried out in an inert atmosphere (argon, nitrogen) with standard Schlenk and dry-box (Vacuum Atmospheres HE-43) techniques. Solvents were purified, dried, and deoxygenated by conventional methods. Light petroleum refers to the fraction boiling between 40 to 60°C. IR data (4000–650 cm⁻¹) were obtained with a Perkin Elmer 1600 FTIR spectrometer for Nujol mulls sandwiched between NaCl plates. Room temperature (20°C) NMR spectra were recorded on a Bruker AC 200 MHz or AM 300 MHz spectrometer. The chemical shift references were the residual solvent signals ($[\text{D}_6]$ benzene, $\delta_{\text{H}} = 7.15$) or an external solution of $[\text{Yb}(\text{C}_5\text{Me}_5)_2]$ in THF/10% C₆D₆ ($\delta_{\text{Yb}} = 0.0$). For the proton assignments, H2'–H6' refer to the substituent phenyl protons. Metal analyses were by EDTA titration with xylenol orange indicator and hexamine buffer of solutions prepared by digestion of accurately weighed samples in concentrated HNO₃/2% concentrated H₂SO₄, followed by dilution with water. Microanalytical data (C, H) were determined by the Campbell microanalytical service, University of Otago, New Zealand. Lanthanoid elements as powders or distilled metal ingots were obtained from Research Chemicals or Rhône–Poulenc. 2,6-Diphenylphenol was purchased from Aldrich and used as received.

Reaction of europium(Hg) and HOdpp: A thick-walled Carius tube was loaded with europium pieces (0.91 g, 6.0 mmol), mercury (1.93 g, 9.60 mmol), and HOdpp (1.04 g, 4.00 mmol). The tube was evacuated to <10⁻³ Torr, sealed and heated to 200°C. After 48 h, an orange-yellow crystalline solid had formed, intermixed with the residual europium(Hg). The mixture was extracted with warm toluene (50 mL) giving a yellow solution which was evaporated to dryness under vacuum. The resulting solid was then recrystallised from toluene/light petroleum (4:1) and gave 0.20 g (15% based on HOdpp) of large yellow crystals of $[\text{Eu}_2(\text{Odpp})_4] \cdot (\text{toluene})$, **1**·(PhMe). IR: $\tilde{\nu} = 1583$ m, 1558 w, 1492 m, 1407 s, 1298 w, 1282 s, 1263 s, 1252 m, 1170 w, 1157 w, 1083 m, 1067 m, 1026 w, 1011 w, 849 m, 804 w, 757 s, 746 s, 734 m, 710 cm⁻¹ vs; MS (70 eV, EI): m/z (%): 246 (100) $[\text{HOdpp}]^+$; no metal-containing ions were detected; C₇₂H₅₂Eu₂O₄·(C₇H₈) (1377.28): calcd C 68.90, H 4.39; found C 69.47, H 4.61. Treatment of the extraction residue with warm toluene (3 × 50 mL), reduction of the combined extracts, and crystallisation gave 0.60 g (44% based on HOdpp, combined yield 59%) of yellow crystals of **1**·(PhMe), which had an IR spectrum identical with that above. C₇₂H₅₂Eu₂O₄·(C₇H₈) (1377.28): calcd Eu 22.07; found Eu 22.17.

Reaction of ytterbium(Hg) and HOdpp: A thick-walled Carius tube was loaded with ytterbium powder (1.73 g, 10.0 mmol), mercury (1.93 g, 9.60 mmol) and HOdpp (1.04 g, 4.00 mmol). The tube was evacuated to $<10^{-3}$ Torr, sealed and heated to 200 °C. After 48 h, a dark red crystalline solid had formed, intermixed with the residual ytterbium(Hg). The mixture was extracted with toluene (60 mL) and gave a dark red solution. A red-orange solid remained with the unreacted metal. Further treatment of the latter with warm toluene (40 mL) gave a near-colourless extract, which was discarded. The red toluene solution was evaporated to dryness and the residue was recrystallised from toluene/light petroleum (2:1) and gave 0.21 g (14% based on HOdpp) of dark red crystals of $[\text{Yb}_2(\text{Odpp})_4] \cdot (\text{toluene})_{1.5}$, **2**·(PhMe)_{1.5}. IR: $\tilde{\nu}$ = 1592 m, 1578 w, 1561 w, 1493 m, 1415 s, 1304 m, 1277 w, 1254 m, 1172 w, 1156 w, 1070 m, 1025 w, 1010 w, 859 m, 846 m, 767 s, 745 s, 732 s, 700 cm^{-1} vs; ^1H NMR ($[\text{D}_6]$ benzene): δ = 2.10 (s, $\text{CH}_3(\text{toluene})$), 6.80 (m, 28H, H₄H_{3'}H_{4'}H_{5'}), 7.10 (m, $\text{C}_6\text{H}_5(\text{toluene})$), 7.22 (d, J = 7.5 Hz, 8H, H₃H₅), 7.38 (dd, 3J = 7.8 Hz 4J = 1.8 Hz, 16H, H_{2'}H_{6'}). The compound was not completely soluble in this solvent and the toluene integration was variable. Complete dissolution and satisfactory integration were achieved with $[\text{D}_8]\text{THF}$: δ = 2.31 (s, 4.5H, $\text{CH}_3(\text{toluene})$), 6.39 (t, 3J = 7.4 Hz, 4H, H₄), 7.01 (t, 3J = 7.4 Hz, 16H, H_{3'}, H_{5'}), 7.10 (m, 7.5H, $\text{C}_6\text{H}_5(\text{toluene})$), 7.18 (t, 3J = 7.5 Hz, 16H, H₃H₅, H_{4'}), 7.53 (d, 3J = 8.1 Hz, 16H, H_{2'}, H_{6'}); ^{171}Yb NMR (PhMe, 298 K): δ = 337 ($\Delta\nu_{1,2}$ = 30 Hz); MS (70 eV, EI): m/z (%): 246 (100) $[\text{HOdpp}]^+$; no metal-containing ions were detected; $\text{C}_{72}\text{H}_{52}\text{O}_4\text{Yb}_2 \cdot (\text{C}_7\text{H}_8)_{1.5}$ (1465.51): calcd C 67.62, H 4.40; found C 67.70, H 4.24. The remaining red-orange solid/residual ytterbium(Hg) obtained after toluene extraction of the initial reaction mixture was allowed to stand in approximately 2 mL of toluene for several weeks. A portion of this material was covered in a heavy oil and examined under a microscope, which showed the presence of some red-orange crystals. One of these was selected under heavy oil, examined by single-crystal X-ray diffraction and found to be $[\text{Yb}(\text{Odpp})_4][\text{Yb}_2(\text{Odpp})_3] \cdot (\text{toluene})$, **3**·(PhMe); ^1H NMR ($[\text{D}_8]\text{THF}$): δ = -22.7* (vbrs, 12H, H_{2'}, H_{6'}), -9.59* (brs, 6H, H₃, H₅), -8.88* (brs, 3H, H₄), 2.18 (s, 3H, $\text{CH}_3(\text{toluene})$), 6.36 (t 3J = 7.1 Hz, 4H, H₄), 6.86–7.08 (m, 37H, H_{3'}, H_{4'}, H_{5'}, $\text{C}_6\text{H}_5(\text{toluene})$), 7.45 (d, 3J = 7.2 Hz, 16H, H_{2'}, H_{6'}), 12.34* (brs, 12H, H_{3'}, H_{5'}), 15.61* (brs, 6H, H_{4'}) (* denotes Yb^{III}). From a separate reaction, the red-orange material was extracted with toluene/THF (1:1, 40 mL) to give a bright orange solution. The solvents were removed under vacuum and the residue was treated with toluene/light petroleum (1:2, 60 mL) which gave, after filtration, a red powder and a yellow filtrate. The red powder was twice recrystallised from toluene/light petroleum (2:1) and gave 0.38 g (26% based on HOdpp) of dark red crystals of **2**·(PhMe)_{1.5}. IR and ^1H NMR spectra were identical with those above. $\text{C}_{72}\text{H}_{52}\text{O}_4\text{Yb}_2 \cdot (\text{C}_7\text{H}_8)_{1.5}$ (1465.51): calcd Yb 23.62; found Yb 24.94. The yellow filtrate was concentrated and cooled and gave 0.23 g (19% based on HOdpp) of yellow crystals of $[\text{Yb}(\text{Odpp})_3]$. IR, visible/near IR and mass spectra were in agreement with those reported.^[4a] ^1H NMR ($[\text{D}_8]\text{THF}$): δ = -22.8 (vbrs, 12H, H_{2'}, H_{6'}), -9.5 (brs, 6H, H₃, H₅), -8.8 (brs, 3H, H₄), 12.4 (brs, 12H, H_{3'}, H_{5'}), 15.7 (brs, 6H, H_{4'}); $\text{C}_{54}\text{H}_{39}\text{O}_3\text{Yb}$ (908.95): calcd C 71.36, H 4.32; found C 71.14, H 4.96.

X-ray crystallography: Single crystals of **1**·(PhMe) and **2**·(PhMe)_{1.5} were grown by slow cooling to room temperature of hot saturated toluene/light petroleum solutions. Representative crystals were selected and mounted under argon in sealed glass capillaries. Intensity data were collected with an Enraf–Nonius CAD-4 diffractometer (graphite-monochromated MoK_α radiation λ = 0.71073 Å) at room temperature. For **3**, a portion of the residue, after toluene extraction of the Yb(Hg)/HOdpp reaction mixture, was covered in viscous oil and a crystal was selected and placed immediately into the cold nitrogen stream of an Enraf–Nonius CCD diffractometer. Crystal and refinement data are listed in Table 5. Crystallographic data

Table 5. Crystal and data collection parameters for **1** to **3**.

	1 ·(PhMe)	2 ·(PhMe) _{1.5}	3 ·(PhMe)
formula	$\text{C}_{79}\text{H}_{60}\text{Eu}_2\text{O}_4$	$\text{C}_{82.5}\text{H}_{64}\text{O}_4\text{Yb}_2$	$\text{C}_{133}\text{H}_{99}\text{O}_7\text{Yb}_3$
M_r	1377.27	1465.50	2328.36
crystal system	monoclinic	triclinic	triclinic
space group	$P2_1/c$ (No. 14)	$P\bar{1}$ (No. 2)	$P\bar{1}$ (No. 2)
a [Å]	18.104(6)	20.16(2)	16.3393(8)
b [Å]	15.234(6)	18.75(1)	16.7399(5)
c [Å]	21.728(12)	17.098(8)	19.1195(9)
α [°]	90	91.48(4)	88.836(2)
β [°]	91.01(4)	90.57(7)	83.840(1)
γ [°]	90	92.03(7)	89.150(2)
V [Å ³]	5992(4)	6457(9)	5197.8(3)
Z	4	4	2
diffractometer	Enraf–Nonius CAD-4	Enraf–Nonius CAD-4	Enraf–Nonius CCD
T (K)	295	295	123
ρ_{calcd} [g cm^{-3}]	1.522	1.507	1.488
$\mu(\text{MoK}_\alpha)$ [cm^{-1}]	21.3	29.3	27.36
crystal size (mm)	$0.95 \times 0.55 \times 0.70$	$0.45 \times 0.32 \times 0.10$	$0.33 \times 0.10 \times 0.08$
$2\theta_{\text{max}}$ [°]	50	50	56.6
unique reflns	10534	22692	24311
reflns observed ($I > 3\sigma(I)$)	8885	7038	10535
$A_{\text{min,max}}^*$	2.21, 2.73	1.34, 2.65	N/A
R	0.032	0.091	0.054
R_w	0.041	0.100	0.051

(excluding structure factors) for the structures reported in this paper have been deposited with the Cambridge Crystallographic Data Centre as supplementary publication nos. CCDC-105133 (**1**·(PhMe)), 105066 (**2**·(PhMe)_{1.5}) and 105082 (**3**·(PhMe)). Copies of the data can be obtained free of charge on application to CCDC, 12 Union Road, Cambridge CB12 1EZ (UK) (Fax: (+44) 1223-336-033; e-mail: deposit@ccdc.cam.ac.uk).

Acknowledgments

We are grateful to the Australian Research Council for support.

- [1] a) H. Schumann, J. A. Meese-Marktscheffel, L. Esser, *Chem. Rev.* **1995**, *95*, 865–986; b) F. T. Edelmann in *Comprehensive Organometallic Chemistry*, 2nd ed. (Eds.: G. Wilkinson, F. G. A. Stone, E. W. Abel), Pergamon, Oxford, **1994**, Chapter 2; c) F. A. Hart in *Comprehensive Coordination Chemistry* (Eds.: G. Wilkinson, R. D. Gillard, J. A. McLeverly), Pergamon, Oxford, **1987**, Chapter 39; d) M. N. Bochkarev, L. N. Zakharov, G. S. Kalinina, *Organoderivatives of the Rare Earth Elements*, Kluwer Academic, Dordrecht, **1995**; e) Herrmann–Brauer, *Synthetic Methods of Organometallic and Inorganic Chemistry*, 3rd ed. (Ed.: W. A. Herrmann), Vol. 6: *Lanthanides and Actinides* (Ed.: F. T. Edelmann), G. Thieme, Stuttgart, **1996**; f) F. T. Edelmann, *Coord. Chem. Rev.* **1994**, *137*, 403–481; g) R. C. Mehrotra, A. Singh, U. M. Tripathi, *Chem. Rev.* **1991**, *91*, 1287–1303; h) D. C. Bradley, *Chem. Rev.* **1989**, *89*, 1317–1322; i) W. J. Evans, *New J. Chem.* **1995**, *19*, 525–533; j) L. G. Hubert-Pfalzgraf, *New J. Chem.* **1995**, *19*, 727–750.
- [2] a) P. B. Hitchcock, M. F. Lappert, A. Singh, *J. Chem. Soc. Chem. Commun.* **1983**, 1499–1501; b) P. B. Hitchcock, M. F. Lappert, A. Singh, *Inorg. Chim. Acta* **1987**, *139*, 183–184; c) H. A. Stecher, A. Sen, A. Rheingold, *Inorg. Chem.* **1988**, *27*, 1130–1132.
- [3] a) D. M. Barnhart, D. L. Clark, J. C. Gordon, J. C. Huffman, R. L. Vincent, J. G. Watkin, B. D. Zwick, *Inorg. Chem.* **1994**, *33*, 3487–3497; b) R. J. Butcher, D. L. Clark, S. K. Grambine, R. L. Vincent-Hollis, B. L. Scott, J. G. Watkin, *Inorg. Chem.* **1995**, *34*, 5468–5476.
- [4] a) G. B. Deacon, S. Nickel, P. I. MacKinnon, E. R. T. Tiekink, *Aust. J. Chem.* **1990**, *43*, 1245–1257; b) G. B. Deacon, T. Feng, B. W. Skelton, A. H. White, *Aust. J. Chem.* **1995**, *48*, 741–756.

- [5] a) J. R. van den Hende, P. B. Hitchcock, M. F. Lappert, *J. Chem. Soc. Chem. Commun.* **1994**, 1413-1414; b) J. R. van den Hende, P. B. Hitchcock, S. A. Holmes, M. F. Lappert, *J. Chem. Soc. Dalton Trans.* **1995**, 1435-1439.
- [6] a) S. Okouchi, S. Sasaki, *Bull. Chem. Soc. Jpn.* **1981**, *54*, 2513-2514; b) J. N. Spencer, A. F. Voigt, *J. Phys. Chem.* **1968**, *72*, 464-470.
- [7] W. J. Evans, M. A. Greci, J. W. Ziller, *Inorg. Chem.* **1998**, *37*, 5221-5226.
- [8] a) B. Cetinkaya, P. B. Hitchcock, M. F. Lappert, R. Smith, *J. Chem. Soc. Chem. Commun.* **1992**, 932-934; b) W. J. Evans, M. A. Greci, J. W. Ziller, *J. Chem. Soc. Dalton Trans.* **1997**, 3035-3039; c) W. J. Evans, M. A. Greci, J. W. Ziller, *Chem. Commun.* **1998**, 2367-2368.
- [9] G. B. Deacon, T. Feng, P. C. Junk, B. W. Skelton, A. H. White, *Chem. Ber.* **1997**, *130*, 851-857.
- [10] W. J. Evans, W. G. McClelland, M. A. Greci, J. W. Ziller, *Eur. J. Solid State Inorg. Chem.* **1996**, *33*, 145-156.
- [11] J. R. van den Hende, P. B. Hitchcock, S. A. Holmes, M. F. Lappert, W.-P. Leung, T. C. W. Mak, S. Prashar, *J. Chem. Soc. Dalton Trans.* **1995**, 1427-1433.
- [12] R. D. Shannon, *Acta Crystallogr. Sect. A*, **1976**, *32*, 751-767.
- [13] a) G. B. Deacon, Q. Shen, *J. Organomet. Chem.* **1996**, *511*, 1-17; b) F. G. N. Cloke, *Chem. Soc. Rev.* **1993**, *22*, 17-24; c) H. Liang, Q. Shen, S. Jin, Y. Lin, *J. Chem. Soc. Chem. Commun.* **1992**, 480-481.
- [14] a) D. L. Clark, G. B. Deacon, T. Feng, R. V. Hollis, B. L. Scott, B. W. Skelton, J. G. Watkin, A. H. White, *J. Chem. Soc. Chem. Commun.* **1996**, 1729-1731; b) G. B. Deacon, T. Feng, P. C. Junk, B. W. Skelton, A. H. White, *J. Chem. Soc. Dalton Trans.* **1997**, 1181-1186.
- [15] C. J. Burns, R. A. Andersen, *J. Am. Chem. Soc.* **1987**, *109*, 915-916.
- [16] J. M. Boncella, T. D. Tilley, R. A. Andersen, *J. Chem. Soc. Chem. Commun.* **1984**, 710-712.
- [17] W. J. Evans, T. A. Ulibarri, *J. Am. Chem. Soc.* **1987**, *109*, 4292-4297.
- [18] C. J. Burns, D. J. Berg, R. A. Andersen, *J. Chem. Soc. Chem. Commun.* **1987**, 272-274.
- [19] C. J. Burns, R. A. Andersen, *J. Chem. Soc. Chem. Commun.* **1989**, 136-137.
- [20] M. N. Bochkarev, V. V. Khramenkov, Y. F. Rad'kov, L. N. Zakharov, *J. Organomet. Chem.* **1992**, *429*, 27-39.

Received: November 4, 1998 [F1426]